The influence of the salt concentration and the diffusion boundary layers on the bi-ionic potential

L. Dammak [a], C. Larchet [a], B. Auclair [a,*], J.A. Manzanares [b], S. Mafé [b]

[a] *Laboratoire des matériaux échangeurs d'ions, Université de Paris-Val de Marne, 94010 Créteil, France*
[b] *Departamento de Termodinámica, Facultad de Física, Universidad de Valencia, E-46100 Burjassot, Spain*

Abstract

Measurements of bi-ionic potential (BIP) across three cation-exchange membranes (CEMs) have been carried out for KCl/CEM/NaCl, KCl/CEM/LiCl, and NaCl/CEM/LiCl systems, where CEM is a polystyrene and divinylbenzene sulfonated membrane (CM2, from Tokuyama Soda), a perfluorosulfonic acid membrane (Nafion® 117, from Du Pont De Nemours) and an heterogenous membrane prepared by inclusion of cation-exchange resin in PVC (CRP, from Rhone Poulenc). The influence of the salt concentration and the diffusion boundary layers (DBLs) on the BIP values has been analysed both theoretically and experimentally. The theoretical model is based on the Nernst–Planck equations, and gives a good description for salt concentrations higher than 5×10^{-4} M. For the CM2 membrane, the DBL thickness changes from 20–23 μm in absence of stirring to 3–4 μm for high stirring rates. Also, the ion diffusion coefficients in this membrane have been estimated to be of the order of 10^{-6} cm^2/s. It has been observed that the counter-ion diffusion coefficients ratio $(\overline{D_A}/\overline{D_B})$ in the membrane increases significantly when the membrane water content decreases, which suggests the possibility of achieving highly selective ion transport with low water content membranes.

Keywords: Bi-ionic potential; Cation-exchange membranes; Diffusion boundary layers; Ion diffusion coefficients; Membrane water content; Stirring effects

1. Introduction

The potential difference which appears between two solutions of different electrolytes (AY and BY) with a common co-ion (Y) at the same concentration separated by a charged membrane is named the bi-ionic potential (BIP). Although the literature concerning this field is extensive [1–13], certain important problems still remain to be clarified. The influence of the diffusion boundary layers (DBLs) on the BIP [14–19] and the concentration dependence of the BIP found in highly charged ion-exchange membranes [13,17,18] are two of them.

The aim of this study is to show that the above questions are interrelated. To this end, we analyse different membrane systems of the form AY/CEM/BY for three cation-exchange membranes (CEMs), with K$^+$, Na$^+$ and Li$^+$ as counter-ions and Cl$^-$ as the common co-ion. The counter-ion A is that of higher diffusion coefficient in solution $(D_A > D_B)$ so that a positive BIP results. The multi-ionic transport through these membrane systems is

* Corresponding author.

considered over a broad range of salt concentrations and stirring rates in the external aqueous solutions. The experimental results are interpreted on the basis of a theoretical model, based on the Nernst–Planck equations, which does not involve the usual assumptions of zero co-ion flux and complete membrane control [1,2,10,13,15,16,20–23]. The first assumption is not valid when the salt concentration approaches the membrane fixed charge concentration, while the second assumption fails even at moderately low concentrations [14]. Therefore, the concentration range where both assumptions could be used is relatively narrow.

The structure of this paper is as follows. First, we review briefly some of theoretical results given previously for the BIP. Then, we present the experimental results obtained, discuss them in the context of the theoretical model developed by Guirao and al. [18], and show the important effects that the DBL exerts on the BIP. These effects are clearly shown by the significant concentration dependence of BIP. Finally, we correlate the ratio of the counter-ion diffusion coefficients in the membrane (obtained under experimental conditions close to membrane control) with the membrane water content.

2. Theory

BIP equations for charged membranes can be derived on the basis of different theoretical approaches: Nernst–Planck equation [22,23], thermodynamics of irreversible processes (TIP) [1,13], Spiegler's friction coefficient model [24], and others [19]. The first studies of BIP made use of the Henderson assumption to integrate the Nernst–Planck equations and found that BIP was related to the ionic mobilities [25] or ionic transference numbers [6,26] but did not change with the external salt concentration. Helfferich's solution of the Nernst–Planck equations [14] with simplifing assumptions (zero co-ion flux, zero water flow, and counter-ion diffusion coefficients ratio in the membrane is constant) leads to two similar equations for the BIP. This former is equal to $(RT/F) \ln(D_A/D_B)$ for complete DBL control, and equal to $(RT/F)\ln(\overline{D_A}/\overline{D_B})$ for complete membrane control. Overbars denote the membrane phase throughout the paper. In a series of
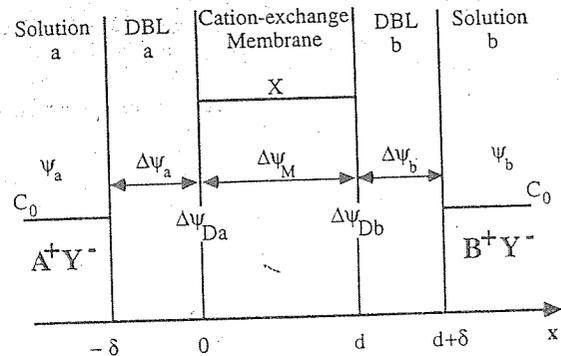

Fig. 1. Schematic view of the bi-ionic system.

elegant papers, Mackey and Meares considered also the Nernst–Planck equation within a quasi-thermodynamic formalism to show the importance of the DBL effects on the ion transport through ion-exchange membranes and the BIP [15,16].

One of the most recent theoretical studies of the BIP using the Nernst–Planck equation is that of Guirao et al. [18]. In that paper, the Nernst–Planck equations were solved, without neglecting the co-ion flux, for a general case where both the membrane and the DBL control the interdiffusion process. The theoretical treatment of BIP is largely based on the electric potential profile proposed by Mackey and Meares for a bi-ionic cell (see Fig. 1 in [15] and Fig. 1 in [16]).

Fig. 1 shows a sketch of the bi-ionic system under study. The transport is considered in the x direction, from $x = -\delta$ to $x = d + \delta$, and all ions are monovalent. The fixed charge concentration of the cation-exchange membrane is denoted by X and its thickness by d. The DBL thickness δ is assumed to be dictated only by the hydrodynamics conditions, following the Nernst layer model [14–16].

The basic equations of the problem are the Nernst–Planck equations

$$J_i = -D_i\left(\frac{dC_i}{dx} + z_i C_i \frac{F}{RT}\frac{d\psi}{dx}\right), \quad i = A,B,Y,$$

$$-\delta < x < 0, d < x < d + \delta \tag{1a}$$

$$\overline{J}_i = -\overline{D}_i\left(\frac{d\overline{C}_i}{dx} + z_i \overline{C}_i \frac{F}{RT}\frac{d\overline{\psi}}{dx}\right), \quad i = A,B,Y,$$

$$0 < x < d \tag{1b}$$

the equation for the (zero) electric current density

$$J_A + J_B - J_Y = 0 \tag{2}$$

and the local electroneutrality equation

$$C_A(x) + C_B(x) = C_Y(x), \quad -\delta < x < 0, \quad d < x < d + \delta \tag{3a}$$

$$\overline{C_A(x)} + \overline{C_B(x)} = \overline{C_Y(x)} + X, \quad 0 < x < d \tag{3b}$$

Here J_i, D_i, and C_i are the flux, diffusion coefficient, and local molar concentration of species i, respectively, and ψ is the local electric potential.

Eqs. (1)–(3) must be solved with the boundary conditions (see Fig. 1).

$$C_A(-\delta) = C_B(d + \delta) = C_0 \tag{4a}$$

$$C_B(-\delta) = C_A(d + \delta) = 0 \tag{4b}$$

Also, according to the well-known Donnan equilibrium [14,22] both the ionic concentration and the electric potential are assumed to be discontinuous at the DBL/membrane interfaces. The concentrations at the inner boundaries of the membrane are related to those at the outer boundaries through the equations

$$\frac{\overline{C_A(0)}}{C_A(0)} = \frac{\overline{C_B(0)}}{C_B(0)} = \frac{\overline{C_Y(0)}}{C_Y(0)} = \frac{X}{2C_Y(0)} + \left[\left(\frac{X}{2C_Y(0)}\right)^2 + 1\right]^{1/2} \tag{5a}$$

and

$$\frac{\overline{C_A(d)}}{C_A(d)} = \frac{\overline{C_B(d)}}{C_B(d)} = \frac{\overline{C_Y(d)}}{C_Y(d)} = \frac{X}{2C_Y(d)} + \left[\left(\frac{X}{2C_Y(d)}\right)^2 + 1\right]^{1/2} \tag{5b}$$

while the electric potential jumps (Donnan potentials) at the interfaces are

$$\Delta\psi_{Da} = \overline{\psi(0)} - \psi(0) = \frac{RT}{F}\ln\frac{\overline{C_Y(0)}}{C_Y(0)} \tag{6a}$$

and

$$\Delta\psi_{Db} = \psi(d) - \overline{\psi(d)} = \frac{RT}{F}\ln\frac{C_Y(d)}{\overline{C_Y(d)}} \tag{6b}$$

Note that ion activity coefficients and single-ion partition coefficients [22] have not been included in the Donnan relationships. This procedure is rather crude, but it gives fairly approximate results [1,22,23] and will allow us to concentrate on the DBL and salt concentration effects on BIP.

The formal solution described in [18] is achieved by transforming Eqs. (1b) into Eq. (7)

$$\frac{J_A}{\overline{D_A}} + \frac{J_B}{\overline{D_B}} + \frac{J_Y}{\overline{D_Y}} = -2\frac{d\overline{C_Y}}{dx} - X\frac{d\overline{\psi}}{dx} \tag{7}$$

which can be integrated to give

$$2\left[\overline{C_Y(d)} - \overline{C_Y(0)}\right] + X\Delta\psi_M + (\overline{j_A} + \overline{j_B} + \overline{j_Y})d = 0 \tag{8}$$

where $\overline{j_i} = \overline{J_i}/\overline{D_i}$ and $\Delta\psi_M = \overline{\psi(d)} - \overline{\psi(0)}$ is the potential drop in the membrane phase. In the DBL, the sum of the Nernst–Planck equations shows that the co-ion concentration gradient is constant (take $X = 0$ in Eq. (7) and consider magnitudes referred to the DBL), and hence

$$C_Y(0) = C_0 - \frac{j_A + j_B + j_Y}{2}d \tag{9a}$$

$$C_Y(d) = C_0 + \frac{j_A + j_B + j_Y}{2}d \tag{9b}$$

where $j_i = J_i/D_i$.

The potential drop in the membrane is easily calculated by adding $(1 - \overline{T})/2$ times Eq. (7) to Eq. (1b) for $i = Y$, with the result

$$\Delta\psi_M = \overline{T}\ln\frac{\overline{C_Y(d)} + X(1 - \overline{T})/2}{\overline{C_Y(0)} + X(1 - \overline{T})/2} \tag{10}$$

The corresponding equations for the DBLs are

$$\Delta\psi_a = \psi(0) - \psi(-d) = \Gamma\ln\frac{C_Y(0)}{C_0} \tag{11a}$$

and

$$\Delta\psi_b = \psi(d + \delta) - \psi(d) = \Gamma\ln\frac{C_0}{C_Y(d)} \tag{11b}$$

where

$$\Gamma = \frac{j_A + j_B - j_Y}{j_A + j_B + j_Y} \tag{12a}$$

84

and

$$T = \frac{\overline{j_A} + \overline{j_B} - \overline{j_Y}}{\overline{j_A} + \overline{j_B} + \overline{j_Y}} \qquad (12b)$$

According to Fig. 1, the BIP is now calculated as the sum of the different potential drops through the system [14–16]

$$BIP = \Delta\psi_a + \Delta\psi_{Da} + \Delta\psi_M + \Delta\psi_{Db} + \Delta\psi_b \qquad (13)$$

The only problem is to know the exact ion fluxes which satisfy the boundary conditions given in Eqs. (4). These fluxes can be obtained either from the solution of two transcendental Eqs. (Eq. (8) and the equivalent equation for one of the cations) [18] or from the numerical integration of the Nernst–Planck equations. Some typical curves of BIP vs. C_0 for different values of d/δ are presented in Fig. 2 of [18]. The BIP values for some interesting limiting cases were also presented there. In particular the BIP is equal to $(RT/F)\ln(D_A/D_B)$ for any value of $d/\delta > 5$ at low concentrations, then goes to a maximum, and finally decreases asymptotically to a fixed value at very high concentrations.

3. Experimental

The experimental set-up employed is shown in Fig. 2 and was described in detail previously [19]. The membrane is sandwiched between two cell compartments, making a seal at the same time. The cell is placed on a stand which centers it with respect to the two watertight magnetic stirrers. The whole de-
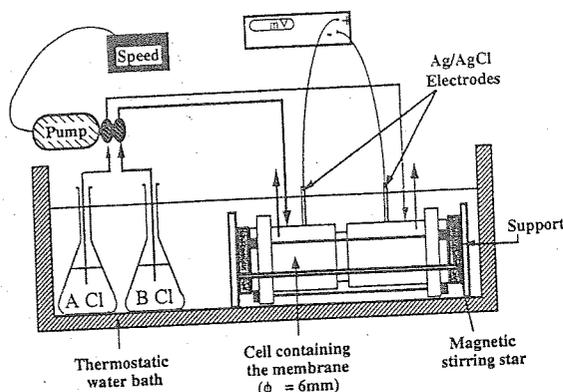
Table 1
Membrane characteristics: exchange capacity C_E, thickness d, water content w, density γ, and fixed charge concentration X

	C_E (meq/g dry membrane)	d (μm)	γ	w (%)	X (M)
CRP	2.10	356	1.26	32	1.80
CM2	1.76	118	1.23	23	1.66
Nafion® 117	0.88	209	1.71	16	1.26

vice is placed in a thermoregulated water bath at $25.0 \pm 0.1°C$, and the circulation of solutions is made by a peristaltic pump equipped with a pair of similar heads of variable speed. The solution inlet is located on the membrane side, while the solution outlet is on the stirring side. The BIP is measured with two silver–silver chloride electrodes [19] and a high input impedance millivoltmeter. All the experimental conditions were similar to those of [19] except for the stirring rate ω, which can now be changed from $\omega_0 = 0$ rpm to $\omega_{max} = 900$ rpm. The BIP measurements were repeated at least twice, and the reproducibility was close to 0.1 mV for the same membrane. For different membranes obtained from the same commercial membrane sample, the difference can rise to 0.5 mV.

The membrane characteristics are given in Table 1. The fixed charge concentration X was calculated by the equation $X = C_E \gamma (1 - w/100)$, where C_E is the exchange capacity, γ is the membrane density, and w (%) is the water content of the membrane. All these characteristics, except for X, are measured according to the French specification [27].

4. Results and discussion

The BIP vs. C_0 plots for the systems KCl/CM2/LiCl, KCl/Nafion® 117/LiCl, KCl/CM2/NaCl, KCl/Nafion® 117/NaCl, NaCl/CM2/LiCl and NaCl/Nafion® 117/LiCl are shown in Fig. 3 (a–f, respectively) for the stirring rates ω_0 and ω_{max}. All the curves show the same shape which deviates from the theoretical one (see Fig. 2 in [18]) only at very low concentrations ($C_0 < 5 \times 10^{-4}$ M). We see also in Fig. 3 (a–f) that the two curves tend to the same BIP value when $C_0 \approx 5 \times 10^{-4}$ M irrespective of the stirring rate ω. This common value appears thus to be a characteristic of

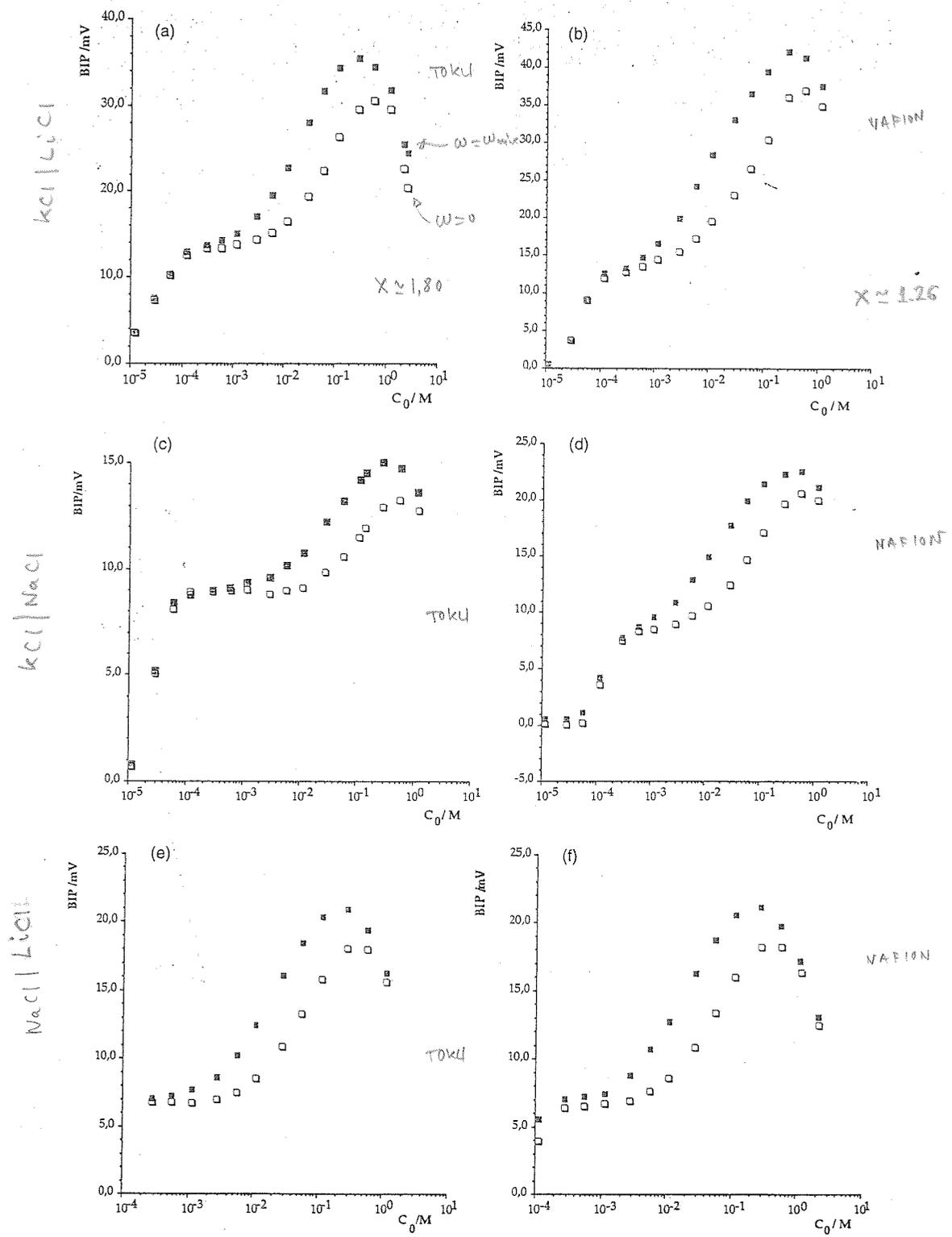Fig. 2. Sketch of the experimental set-up.

Fig. 3.
KCl/N

Fig. 3. Bi-ionic potential versus C_0 for the system (a) KCl/CM2/LiCl, (b) KCl/Nafion® 117/LiCl, (c) KCl/CM2/NaCl, (d) KCl/Nafion® 117/NaCl, (e) NaCl/CM2/LiCl, (f) NaCl/Nafion® 117/LiCl. Stirring rates: $\omega_0 = 0$ rpm (□) and $\omega_{max} = 900$ rpm (▨).

Table 2
Bi-ionic potential values (in mV) for the low concentration limit in Fig. 3 (a–f), where only the domain $C_0 \geq 5 \times 10^{-4}$ M has been considered

	KCl/CM2/ LiCl	KCl/CM2/ NaCl	NaCl/CM2/ LiCl
CM2	13.3	8.7	6.8
Nafion® 117	13.0	8.0	6.2

the salts employed, and is approximately independent of the membrane considered, as is shown in Table 2. It should be emphasized that similar results were obtained by Tasaka for the membrane systems KCl/SC1/NaCl and KCl/SC4/NaCl [13]. This proves that at low concentration the BIP becomes almost independent of the stirring rate and the membrane, and is dictated by the salt diffusion through the DBLs. However, we remark that the experimental values in Table 2 are lower than the theoretical prediction $(RT/F)\ln(D_A/D_B)$, which is equal to 9.9 mV for KCl/CEM/NaCl, 16.5 mV for KCl/CEM/LiCl, and 6.6 mV for NaCl/CEM/LiCl, if the infinite dilution value are introduced for the ion diffusion coefficients [28].

The qualitative behaviour of BIP at low concentrations ($C_0 < 2.5 \times 10^{-4}$ M) is significantly different to that predicted theoretically [18], and should be investigated further. Some possible explanations are:

(i) The existence of a water flow opposing the faster counter-ion diffusion through the membrane. However, at this concentration range, the convection velocity seems to be very small and insufficient to makes a discrepancy of 3.2 mV between $(RT/F)\ln(D_{K^+}/D_{Li^+})$ and its experimental value.

(ii) The ion diffusion coefficients at $C_0 \approx 2.5 \times 10^{-4}$ M differ significantly from those corresponding to infinite dilution.

(iii) The total ion concentration coming from water impurities is not negligible at $C_0 < 2.5 \times 10^{-4}$ M, as can be deduced from the value of the water specific resistivity $\rho = 4.0$ MΩ cm. By using Helfferich's expression [14] for the multi-ionic potential (MIP) of a membrane system under DBL control, we can estimate the electric potential difference at low concentrations as

$$MIP = \frac{RT}{F}\ln\left(\frac{D_A C_0 + I}{D_B C_0 + I}\right) \qquad (14)$$

where $I = \Sigma_j D_j C_j |z_j|$, and subscript j runs over the counter-ions present in the water used for the solutions preparation. Thus the potential difference takes the well-known asymptotic value $(RT/F)\ln(D_A/D_B)$ when $C_0 \geq 10^{-4}$ M (that is, when $C_0 \gg I/D_B$), and tends to zero as $(RT/F)(D_A - D_B)(C_0/I)$ when C_0 decreases to 10^{-6} M–10^{-5} M (that is, when $C_0 \ll I/D_A$). This is indeed what is observed qualitatively in the curves of Fig. 3 (a–d), though Table 2 shows that some quantitative disagreement still exists.

After giving a qualitative explanation of the BIP behaviour at very low concentrations, we will focus on the concentration domain 10^{-3} M $\leq C_0 \leq 2$ M because we are limited by the stability of the Ag/AgCl electrodes at high chloride concentrations [19]. For this concentration range, all the curves of Fig. 3 (a–f) have the shape predicted by the theory [18]. Also, the curves corresponding to ω_{max} are above those obtained with ω_0. This is in good agreement with the theoretical predictions, since we know that the DBL thickness decreases with the stirring rate ω (see Fig. 3 in [15]), and thus d/δ should increase with ω.

In Fig. 4, we have reported the BIP versus C_0 plot obtained for the system KCl/CM2/LiCl at different stirring rates. We have considered only the concentration range 0.1 M $\leq C_0 \leq 1$ M. The maximum of BIP, denoted by BIP_{max}, has been determined for every ω, and the variation of BIP_{max} with ω is shown in Fig. 5. Curves similar to those of Figs. 4 and 5 can also be obtained for the other bi-ionic systems. The general result is that BIP_{max} increases with ω, and tends to an asymptotic value, denoted by BIP_∞, for very high stirring rates. For these high stirring rates, the DBL thickness is reduced to a minimum value (though still different from zero), and the assumption of complete membrane control allows us to estimate BIP_∞ as

$$BIP_\infty \approx \frac{RT}{F}\ln\left(\frac{\overline{D_A}}{\overline{D_B}}\right) \qquad (15)$$

We have plotted the BIP_{max} versus ω for each bi-ionic system and determined $(RT/F)\ln(\overline{D_A}/\overline{D_B})$ from these data. Table 3 correlates the ratio of the counter-ion diffusion coefficients in the membrane with the membrane water content obtained for the different membrane systems. The ratios D_A/D_B
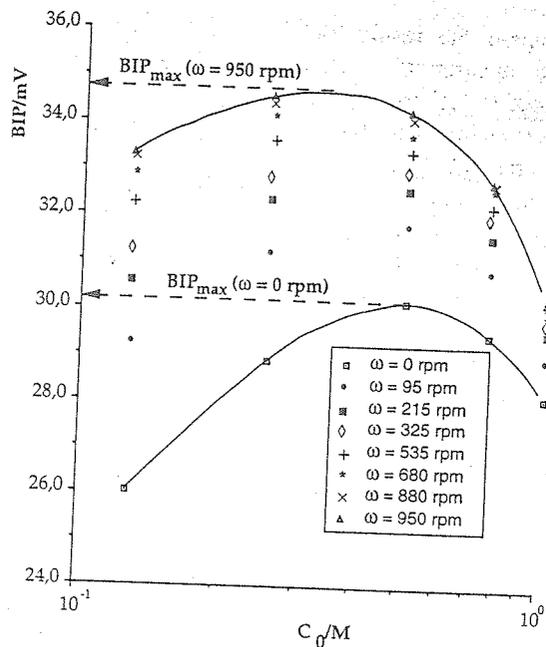
Fig. 4. Bi-ionic potential versus C_0 (0.1 M $\leq C_0 \leq$ 1 M) for the system KCl/CM2/LiCl at different stirring rates ω (rpm).

Table 3
Correlation between the experimental counter-ion diffusion coefficients ratios and the membrane water content

	$\overline{D}_{Na^+}/\overline{D}_{Li^+}$	$\overline{D}_{K^+}/\overline{D}_{Na^+}$	$\overline{D}_{K^+}/\overline{D}_{Li^+}$	w (%)
Aqueous solution (infinite dilution)	1.29	1.47	1.89	
CRP	2.05	1.60	3.10	32
CM2	2.25	1.80	3.95	23
Nafion® 117	2.35	2.35	5.20	16

characteristic of the respective (low concentration) pure aqueous solutions [28] are also shown for the sake of comparison. The important conclusion to be drawn from Table 3 is that the lower the water content, the higher the counter-ion diffusion coefficients ratio in the membrane. Similar trends were advanced recently for polystyrene sulfonic-acid membranes [13,18] and could also be operative in cation-exchange membranes prepared of sulfonate-containing aromatic polyamides [29]. This suggests
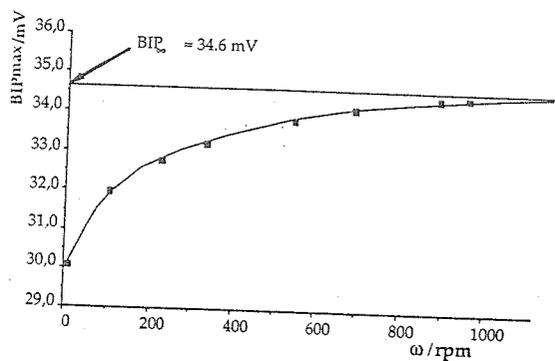
the possibility of achieving highly selective ion transport with membranes having low water contents [13,19,29].

Counter-ion diffusion coefficient ratios very close to those characteristic of pure aqueous solutions have however been reported in some previous studies on BIP [21,30]. This might be ascribed to the higher water content of the membranes employed there and the fact that these ratios were obtained in some cases by applying equations valid only for complete membrane control to situations where a mixed DBL-membrane control was likely to occur.

It should also be emphasized that the ratios shown in Table 3 are "apparent" values, and could be influenced by:

1. The water flow through the membrane, which might be important at high concentrations ($C_0 \geq$ 0.1 M).
2. The membrane preference (if any) for one of the two counter-ions. This preference can be described by introducing the so-called selectivity coefficient [2,14].

Additional experimental work aimed to confirm the results in Table 3 for other low water content membranes would be desirable, since it is often the case that no simple correlation between the ion diffusion coefficients in pure solution and in the membrane is possible due to the differences between these two environments.

Let us mention finally that we can deduce for each membrane in Table 3 a given ratio $\overline{D}_A/\overline{D}_B$ from the two others. Again, the agreement between theory and experiment shows that the assumption of complete membrane control is approximately valid for high concentrations and stirring rates.

Fig. 5. BIP$_{max}$ versus the stirring rate ω (rpm) for the system KCl/CM2/LiCl.

We have used an iterative method to estimate the absolute value of the diffusion coefficients. First, we introduce some initial values for $\overline{D_A}$ and $\overline{D_Y}$ and obtain $\overline{D_B}$ from Table 3. Second, we compute the BIP versus C_0 curves for different values of δ in the range 1 μm $\leq \delta \leq 50$ μm, and, for every stirring rate, we accept that DBL thickness which gives the observed value of BIP_{max}. Then, we solve numerically Eqs. (1)–(3) with all these initial parameters,

compare the results obtained to the experimental data, and modify the parameters accordingly. This procedure is repeated until a good agreement between theory and experiment is achieved. Generally a series of two or three iterations proves to be enough, since we know qualitatively how the BIP depends on $\overline{D_A}$ and $\overline{D_Y}$. The final results obtained for the CM2 membrane are shown in Table 4. Fixed charge concentration and membrane thickness were
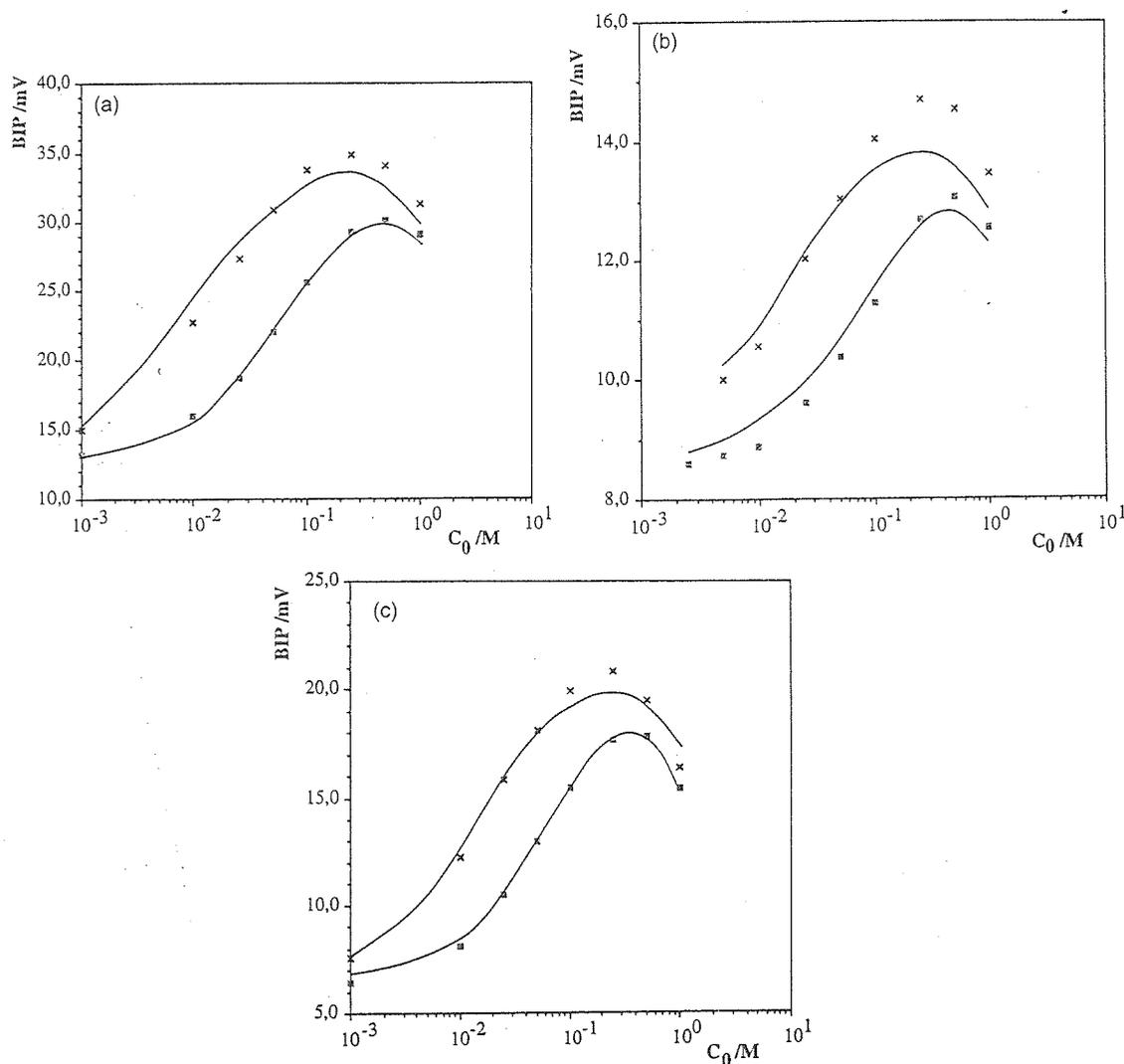

Fig. 6. Experimental data (points) and theoretical predictions (continuous lines) of BIP versus C_0 ($C_0 \geq 10^{-3}$ M) for the bi-ionic system (a) KCl/CM2/LiCl, (b) KCl/CM2/NaCl, (c) NaCl/CM2/LiCl. Stirring rates: $\omega_0 = 0$ rpm (■) and $\omega_{max} = 900$ rpm (×).

Table 4
Ion diffusion coefficients for the CM2 membrane. The DBL thickness values are 3–4 μm at ω_{max} and 20–23 μm at ω_0

	KCl/CM2/ LiCl	KCl/CM2/ NaCl	NaCl/CM2/ LiCl
$\overline{D_A}$ (10^{-6} cm^2/s)	3.00	3.00	1.72
$\overline{D_B}$ (10^{-6} cm^2/s)	0.76	1.72	0.76
$\overline{D_Y}$ (10^{-6} cm^2/s)	0.99	0.99	0.99

those given in Table 1. The order of magnitude of the values introduced for the Nafion® 117 membrane was similar to those in Table 4.

In Fig. 6 (a–c) we report both the experimental points and the theoretical results (continuous lines) obtained by using the numerical values in Table 4. We emphasize the following points:

(i) There is a reasonable agreement between the theoretical and experimental results (differences between them are lower than 10% in all cases). Since the theory incorporates both the DBLs and the CEM, we conclude that for the external salt concentration range 5×10^{-4} M $\leq C_0 \leq$ 1 M, ion transport occurs with a mixed DBL-membrane control. In fact, if only a membrane control or DBLs control is considered, theoretical treatments show that BIP must decrease with C_0 and reaches two different asymptotic limits for the case of high and low values of C_0, respectively [1,23], which is not the case of our experiments.

(ii) As expected, the DBL thickness is approximately independent of the counter-ion nature though it is very sensitive to the hydrodynamics conditions. For ω_0, where only the solution circulation is maintained with a flow rate of 800 ml/h, $\delta \approx 20$ μm. This value is in the range of those obtained by Mackey and Meares [15], Ktari [31] and Dieye [32]. On the other hand, the DBL thickness obtained for ω_{max} is about 4 μm, which is lower than some of the thicknesses reported by other authors for high agitation [15,31,32]. This difference may be due either to the very high stirring and circulation flow rates used here or to some untraced error in the parameter assignment procedure employed. Since it is known that the use of solution jets directed towards the membrane surface [19] reduces significantly the value of δ (which can be of the order of 1–10 μm [2,33]), we could discard the latter possibility.

(iii) The order of magnitude of the ion diffusion coefficients in the membrane (10^{-6} cm^2/s) is the typical one found for ion-exchange membranes [14,34,35]. The series $\overline{D_{K^+}} > \overline{D_{Na^+}} > \overline{D_{Li^+}}$ obtained for the different membranes coincides with that characteristic of an aqueous solution, which confirms that hydration plays also a fundamental role in the ion transport through the membrane [14,34].

Additional experiments aimed at determining the counter-ion membrane selectivity and the water flow effects on BIP are in progress. (Note: The C/Macintosh software is available from authors [a], whereas the Fortran software is available authors [b].)

5. List of symbols and abbreviations

	(variables with overbars in the text refer to membrane phase)
BIP	bi-ionic potential (mV)
C_0	concentration of the two bulk solutions a and b (M)
C_E	exchange capacity (meq g^{-1} dry membrane in the H$^+$ form)
CEM	cation-exchange membrane
C_i	local molar concentration of ion i (M)
d	membrane thickness (μm)
DBL	diffusion boundary layer
D_i	diffusion coefficient of ion i (cm^2 s^{-1})
F	Faraday constant (C mol^{-1})
I	variable characteristic of the water impurity (mol cm^{-1} s^{-1})
J_i	flux of ion i (mol cm^{-2} s^{-1})
j_i	reduced flux of ion i (mol cm^{-4})
MIP	multi-ionic potential (mV)
R	gas constant (J mol^{-1} K^{-1})
T	absolute temperature (K)
v	convection velocity (cm s^{-1})
w	membrane water content (%)
X	membrane fixed charge concentration (M)
x	position
z_i	charge number of ion i

5.1. Greek symbols

δ	diffusion boundary layer thickness (μm)
$\Delta\psi_{Dj}$	Donnan potential at the interface between the membrane and solution j (mV)

$\Delta\psi_j$ potential drop in the diffusion boundary layer of solution j (mV)

$\Delta\psi_M$ potential drop in the membrane phase (mV)

γ membrane density

ρ water resistivity ($M\Omega$ cm)

ω stirring rate (rpm)

ψ local electric potential (mV)

References

[1] M. Tasaka, S. Iwaoka, K. Yamagishi and Y. Ikeda, Dependence of bi-ionic potential across membranes on salt concentration, J. Membrane Sci., 24 (1985) 29.

[2] F. Helfferich, Bi-ionic potentials, Discuss. Faraday Soc., 21 (1956) 83.

[3] F. Bergsma and A.J. Staverman, Bi-ionic potentials, Discuss. Faraday Soc., 21 (1956) 61.

[4] G. Scatchard and F. Helfferich, The effect of stirring on cells with cation-exchange membranes, Discuss. Faraday Soc., 21 (1956) 70.

[5] M.R.J. Wyllie, Ion-exchange membranes. I. Equations for the multi-ionic potential, J. Phys. Chem., 58 (1954) 67.

[6] K. Sollner, The origin of bi-ionic potentials across porous membranes of high ionic selectivity, J. Phys. Chem, 53 (1949) 1211.

[7] K. Kaibara and H. Kimizuka, Multi-ionic potential and membrane permeability matrix. I. NaCl–CsCl bi-ionic system with a cation-exchange membrane, Bull. Chem. Soc. Jpn., 55(6) (1982) 1743.

[8] K. Kaibara, H. Inoue and H. Kimizuka, Multi-ionic potential and membrane permeability matrix. II. Na^+–Ca_2^{2+} bi-ionic system with a cation-exchange membrane and effects of Cl^- on cation transport, Bull. Chem. Soc. Jpn., 60 (1987) 3175.

[9] K. Kaibara, H. Inoue and T. Aritomi, Multi-ionic potential and membrane permeability matrix. III. Diffusion and concentration of ions within membrane phase as a controlling factor to ion permselectivity, Bull. Chem. Soc. Jpn., 62 (1989) 2362.

[10] Y. Toyoshima and H. Nozaki, Bi-ionic potential across charged membranes, J. Phys. Chem., 74 (1970) 2704.

[11] D.K. Hale and K.P. Govindan, Bi-ionic potentials with sulfonic and phosphonic acid cation-exchange membranes, J. Electrochem. Soc., 166 (1969) 1373.

[12] K. Nomura, A. Matsubara and H. Kimizuka, Bi-ionic potential across liquid membranes with some anionic surfactants, Bull. Chem. Soc. Jpn., 58 (1985) 277.

[13] M. Tasaka, H. Sugioka, M. Kamaya, T. Tanaka, S. Suzuki and Y. Ogawa, Dependence on salt concentration of bi-ionic potential across polystyrene sulfonic-acid type membranes J. Membrane Sci., 38 (1988) 27.

[14] F. Helfferich, Ion Exchange, McGraw-Hill, New York, 1962.

[15] D. Mackey and P. Meares, On the correction for unstirred solution films in ion-exchange membrane cells, Kolloid-Z., 167 (1959) 31.

[16] D. Mackey and P. Meares, Ion-exchange across a cationic membrane in dilute solutions, Kolloid-Z., 171 (1960) 139.

[17] D. Mackey and P. Meares, Ion-exchange across a cationic membrane in concentrated solutions, Kolloid-Z., 176 (1961) 23.

[18] A. Guirao, S. Mafé, J.A. Manzanares and J.A. Ibáñez, Bi-ionic potential of charged membranes: effects of the diffusion boundary layers, J. Phys. Chem. 99 (1995) 3387.

[19] L. Dammak, C. Larchet, B. Auclair, V.V. Nikonenko, V.I. Zabolotsky, From the multi-ionic to the bi-ionic potential, Eur. Polym. J., in press.

[20] K. Inenaga and N. Yoshida, Effect of an unstirred layer on ion transport through a membrane, J. Membrane Sci., 6 (1980) 271.

[21] F.A. Siddiqui and N.I. Alvi, Transport studies with parchment supported model membranes, J. Membrane Sci., 46 (1989) 185.

[22] R.P. Buck, Kinetics of bulk and interfacial ionic motion: microscopic bases and limits for the Nernst–Planck equation applied to membrane systems, J. Membrane Sci., 17 (1984) 1.

[23] J. Pellicer, S. Mafé and V.M. Aguilella, Ionic transport across porous charged membranes and the Goldman constant field assumption, Ber. Bunseng. Phys. Chem., 90 (1986) 867.

[24] K.S. Spiegler, Transport process in ionic membranes, Trans. Faraday Soc., 54 (1958) 1408.

[25] L. Michaelis, The permeability of membranes, Nature, 13 (1926) 33.

[26] H.P. Gregor and K. Sollner, Improved methods of preparation of electropositive "permselective" protamine collodion membranes, J. Phys. Chem., 50 (1946) 88.

[27] AFNOR, Séparation d'ions en phase liquide; Membranes polymères échangeuses d'ions; Caractéristiques et méthodes d'essais des membranes homopolaires, NF X45-200, 1995.

[28] R.A. Robinson and R.H. Stokes, Electrolyte Solutions, Butterworths, London, 1959.

[29] Yu.E. Kirsh, N.V. Yanul', I.M. Malkina, Yu.A. Fedotov and S.F. Timashev, Selective ionic transport in cation-exchange membranes prepared of sulfo-containing polyamides of various composition, Russ. J. Electrochem., 31 (1995) 7.

[30] S.K. Saharay and A.S. Basu, BIP measurements with Neosepta membranes (cation exchangers) for some univalent and bivalent cation pairs in electrolytic solutions, Indian J. Technol., 17 (1979) 423.

[31] T. Ktari, Contribution à l'étude de la dialyse ionique croisée, Thesis, University Paris-XII, 1992.

[32] A.L. Dieye, Etude de la défluoration des eaux par dialyse ionique croisée, Thesis, University Paris-XII, 1995.

[33] H.P. Gregor and D.M. Wetstone, Specific transport across sulphonic and carboxylic interpolymer cation-selective membrane, Discuss. Faraday Soc., 21 (1956) 162.

[34] T. Xue, R.B. Longwell and K. Osseo-Asare, Mass transfer in Nafion membrane system: Effect of ionic size and charge on selectivity, J. Membrane Sci., 58 (1991) 175.

[35] H.L. Yeager and A. Steck, Cation and water diffusion in Nafion ion exchange membranes: influence of polymer structure, J. Electrochem. Soc., 128 (1981) 1880.